

# A numerical study of the Random Dimerized XX spin-1/2 chain

P. Henelius and S.M. Girvin

*Department of Physics, Indiana University, Bloomington, IN 47405*

(May 2, 2019)

The effects of randomness and dimerization on the spin-1/2 XX chain are studied by a mapping to free fermions. Results are presented for the transverse and longitudinal components of the average and typical spin and string correlation functions. Contrary to previous numerical evidence, the decay exponents of all the above correlation functions are found to be in good agreement with the theoretical RG predictions for the random singlet phase. We also present cross-over functions for the above correlation functions in the random dimer phase. Disorder averages have been taken for system sizes up to  $N=1024$ , about ten times larger than in previous studies.

## I. INTRODUCTION

It is the purpose of this work to study the effects of disorder and dimerization on the ground state of the XX spin-1/2 chain. Much analytical<sup>1-9</sup> and numerical<sup>10-14</sup> work has been done on random spin chains, as well as higher dimensional spin models<sup>15-17</sup> and to begin with we will review some of the knowledge we have of these systems.

In 1983 Haldane pointed out<sup>18</sup> that integer spin chains have an energy gap, while half integer spin chains are gapless. If we introduce alternating bond strength in a spin-1/2 chain, and thereby enforce dimerization, an energy gap is induced<sup>19</sup>. In the absence of disorder the spin-1 and dimerized spin-1/2 chains are in the same phase<sup>12</sup>, since one can be continuously transformed into the other. This Haldane phase is characterized by an excitation gap, exponential decay of the spin correlation function and a non-vanishing string order parameter, to be defined below.

Fisher<sup>1-3</sup> has recently made considerable progress towards understanding the strongly disordered random singlet (RS) phase of the spin chain. Through an asymptotically exact RG scheme closely related to that of Dasgupta and Ma,<sup>20</sup> he showed that the RS phase is characterized by a dynamic critical exponent  $z = \infty$ , meaning that the characteristic time scale is not a power of the characteristic length scale, but rather an exponential function, giving so-called activated dynamics. The RS phase has no energy gap and the spin correlation function between two given sites vary over several orders of magnitude from one disorder configuration to the next. The average spatial decay of the spin correlation functions are, however, described by power laws<sup>2</sup>. Due to the broad distributions, the typical correlations (the average of the logarithm of the correlation function) behave very differently from the average correlation functions. No string order exists. In the RS phase all the spins pair up and form singlets over arbitrarily large distances. Average correlation functions are dominated by these strong pair-wise coupling of spins, and due to the singlet nature of the pairing, all components of the correlation functions are predicted to decay with the same exponent, even if the underlying Hamiltonian is not rotationally invariant. If a weak dimerization is now enforced the system is driven

to a random dimer (RD) phase which is gapless, like the RS phase, but which has a non-vanishing string order<sup>4</sup>, like the Haldane phase.

Recently Young and Rieger<sup>10</sup> were able to numerically verify many of these striking RG predictions by using a mapping to free fermions. In this paper we have extended their results to larger system sizes and we have studied additional correlation functions in the RS and RD phases. Different components of the correlation functions are found to decay with the same exponents, in agreement with theoretical RG predictions, but contrary to earlier numerical work<sup>11</sup>. In the RD phase we present the full finite size scaling cross-over functions for the average and typical values of both components of the spin and string correlation functions.

## II. MODEL

We consider the following Hamiltonian  $H$  of the XX chain:

$$H = \sum_{i=1}^N J_i (S_i^x S_{i+1}^x + S_i^y S_{i+1}^y) \quad (1)$$

where  $S_i^\alpha$  are spin-1/2 operators obeying periodic boundary conditions ( $\vec{S}_{N+1} = \vec{S}_1$ ) and  $J_i$  are positive coupling constants.

In the disordered system we present results for the following flat bond distributions:

$$\begin{aligned} P(J_o) &= (2+d)^{-1} \theta(2+d-J_o) \theta(J_o), \\ P(J_e) &= (2-d)^{-1} \theta(2-d-J_e) \theta(J_e), \end{aligned} \quad (2)$$

where  $J_o$  and  $J_e$  denote odd and even bonds. The dimerization is defined as

$$\delta = \frac{[\ln J_o]_{\text{av}} - [\ln J_e]_{\text{av}}}{\text{var}[\ln J_o] + \text{var}[\ln J_e]}, \quad (3)$$

where var denotes variance. In terms of the above distributions this reduces to

$$\delta = \frac{1}{2} \ln \left( \frac{2+d}{2-d} \right) \quad (4)$$

In the disorder free dimerized system  $J_o = 1 - d/2$  and  $J_e = 1 + d/2$  and we use Eq. (4) to define the dimerization  $\delta$ .

The longitudinal component of the spin correlation function,  $C^z(r)$ , is defined as

$$C^z(r) = \frac{4}{N} \sum_{i=1}^N \langle S_i^z S_{i+r}^z \rangle. \quad (5)$$

The transverse component,  $C^x(r)$ , is defined analogously.

The longitudinal component of the string correlation function,  $O^z(r)$ , is defined as

$$O^z(r) = -\frac{4}{N} \sum_{i=1}^N \langle S_i^z \exp[i\pi(S_{i+1}^z + S_{i+2}^z + \dots + S_{i+r-1}^z)] S_{i+r}^z \rangle. \quad (6)$$

Using the identity  $S^z = \exp(i\pi S^z)/2i$  this can be rewritten, for spin-1/2 operators and  $r$  odd as

$$O^z(r) = \frac{2^{r+1}}{N} \sum_{i=1}^N \langle S_i^z S_{i+1}^z \dots S_{i+r}^z \rangle. \quad (7)$$

The behavior of the string correlation function in a dimerized system depends on whether the site index  $i$  in the sum above is odd or even. Therefore we have separated the above expression into a sum over even sites, defining  $O_e^z(r)$  as

$$O_e^z(r) = \frac{2^{r+2}}{N} \sum_{i \text{ even}} \langle S_i^z S_{i+1}^z \dots S_{i+r}^z \rangle, \quad (8)$$

and a sum over odd sites, defining  $O_o^z(r)$  as

$$O_o^z(r) = \frac{2^{r+2}}{N} \sum_{i \text{ odd}} \langle S_i^z S_{i+1}^z \dots S_{i+r}^z \rangle. \quad (9)$$

The difference between the the expressions is denoted  $O_d^z(r) = O_o^z(r) - O_e^z(r)$ . The transverse component of the string order function  $O^x$  is defined analogously.

This correlation function was introduced<sup>21-23,12</sup> to measure hidden long-range correlations in integer spin chains where the ordinary spin-spin correlation function vanishes exponentially. If we, for example have a perfectly dimerized spin chain with  $J_{2i} = \infty$  and  $J_{2i+1} = 0$ , then the spins form singlets around the strong bonds, and neighboring singlets are uncorrelated, with  $O_d^z = O_o^z = 1$  and  $O_e^z = 0$ . If, on the other hand there is no dimerization in the system  $O_e^z = O_o^z = O^z$  and hence  $O_d^z = 0$ . The string order parameter  $O_{str}^z$  is defined as

$$O_{str}^z = \lim_{r \rightarrow \infty} O_o^z(r) = \lim_{r \rightarrow \infty} O_d^z(r). \quad (10)$$

We are, however, working with finite size systems with periodic boundary conditions and all results are calculated at the largest distance around the ring. Results for

$C^x(r)$  are calculated at  $r = N/2$ .  $C^z(r)$  vanishes for  $r$  even (see Appendix) and so results are for  $r = N/2 - 1$ . Both components of the string order function are defined for odd  $r$ , and they are calculated at  $r = N/2 - 1$ , using our definition of the correlation functions. For simplicity we have, however, plotted all results as a function of  $n = N/2$ . This will introduce some corrections to scaling for  $C^z$  and will be discussed below.

All decay exponents  $\theta$  are defined according to

$$f(r) \propto r^{-\theta}. \quad (11)$$

### III. MAPPING TO FREE FERMIONS

Using the Jordan-Wigner transformation we can map the XX model onto free fermions<sup>24</sup>. Therefore we only need to solve the one-body problem which involves diagonalizing a  $(N \times N)$  matrix and hence we can study fairly large system sizes, up to about  $N = 2048$  for a clean system, and up to  $N = 1024$  when disorder averages are taken over several thousand configurations.

We apply the Jordan-Wigner transformations

$$\begin{aligned} S_i^- &= \exp(-i\pi \sum_{j=1}^{i-1} c_j^\dagger c_j) c_i \\ S_i^+ &= c_i^\dagger \exp(i\pi \sum_{j=1}^{i-1} c_j^\dagger c_j) \end{aligned} \quad (12)$$

to our Hamiltonian and obtain

$$H = \sum_{i=1}^N \frac{J_i}{2} [c_i^\dagger c_{i+1} + c_i c_{i+1}^\dagger]. \quad (13)$$

Next we must calculate the string correlation function in the fermion language:

$$\begin{aligned} \prod_{j=i}^{i+r} S_j^z &= \prod_{j=i}^{i+r} (c_j^\dagger c_j - \frac{1}{2}) \\ &= \left(\frac{-1}{2}\right)^{r+1} \prod_{j=i}^{i+r} (1 - 2c_j^\dagger c_j) \\ &= \left(\frac{-1}{2}\right)^{r+1} \prod_{j=i}^{i+r} (c_j^\dagger + c_j)(c_j^\dagger - c_j) \end{aligned} \quad (14)$$

We proceed by rewriting this<sup>10,25</sup> in the form

$$\prod_{j=i}^{i+r} S_j^z = \left(\frac{-1}{2}\right)^{r+1} \prod_{j=i}^{i+r} A_j B_j. \quad (15)$$

where  $A_j = (c_j^\dagger + c_j)$  and  $B_j = (c_j^\dagger - c_j)$ . This expression is easily evaluated using Wick's theorem. First we can show that

$$\langle A_i A_j \rangle = \delta_{ij} \quad (16)$$

$$\langle B_i B_j \rangle = -\delta_{ij} \quad (17)$$

$$\langle B_i A_j \rangle = \langle B_j A_i \rangle = -\delta_{ij} + 2\langle c_j^\dagger c_i \rangle \quad (18)$$

$$\langle A_j B_i \rangle = -\langle B_i A_j \rangle = \delta_{ij} - 2\langle c_j^\dagger c_i \rangle \quad (19)$$

and the only non-zero contractions to appear are then of the form  $\langle A_j B_i \rangle$  or  $\langle B_j A_i \rangle$ . This leads to the following determinant:

$$\left\langle \prod_{j=i}^{i+r} S_j^z \right\rangle = \left(\frac{-1}{2}\right)^{r+1} \times \begin{vmatrix} \langle A_i B_i \rangle & \langle A_i B_{i+1} \rangle & \cdots & \langle A_i B_{i+r} \rangle \\ \langle A_{i+1} B_i \rangle & \langle A_{i+1} B_{i+1} \rangle & \cdots & \langle A_{i+1} B_{i+r} \rangle \\ \vdots & \vdots & \ddots & \vdots \\ \langle A_{i+r} B_i \rangle & \langle A_{i+r} B_{i+1} \rangle & \cdots & \langle A_{i+r} B_{i+r} \rangle \end{vmatrix}. \quad (20)$$

Care has to be taken since the fermion creation and annihilation operators obey periodic boundary conditions when  $N/2$  is odd and antiperiodic boundary conditions when  $N/2$  is even.

All that remains to do is to calculate  $\langle A_i B_j \rangle$ . We find the unitary transformation  $U$  that diagonalizes the Hamiltonian:

$$\begin{aligned} d_i^\dagger &= \sum_j c_j^\dagger U_{ji} & c_i^\dagger &= \sum_j d_j^\dagger U_{ij} \\ d_i &= \sum_j c_j U_{ji} & c_i &= \sum_j d_j U_{ij}, \end{aligned} \quad (21)$$

where  $c_i^\dagger$  denotes a fermion creation operator in the old basis and  $d_i^\dagger$  denotes a creation operator in the new basis. Then we find that

$$\langle c_i^\dagger c_j \rangle = \left\langle \sum_k d_k^\dagger d_k U_{ik} U_{jk} \right\rangle, \quad (22)$$

and in the ground state

$$\langle c_i^\dagger c_j \rangle = \sum_{k < k_F} U_{ik} U_{jk}. \quad (23)$$

Hence

$$\langle A_i B_j \rangle = \delta_{ij} - 2 \sum_{k < k_F} U_{ik} U_{jk}. \quad (24)$$

This completes the expression for the longitudinal component of the string correlation function as a determinant. The equivalent expression for the other correlation functions are obtained in a very similar way<sup>25</sup> and we only state the results. The transverse component of the string correlation function is

$$\left\langle \prod_{j=i}^{i+r} S_j^x \right\rangle = \left(\frac{-1}{2}\right)^{r+1} \times \begin{vmatrix} \langle B_i A_{i+1} \rangle & \langle B_i A_{i+3} \rangle & \cdots & \langle B_i A_{i+r} \rangle \\ \langle B_{i+2} A_{i+1} \rangle & \langle B_{i+2} A_{i+3} \rangle & \cdots & \langle B_{i+2} A_{i+r} \rangle \\ \vdots & \vdots & \ddots & \vdots \\ \langle B_{i+r-1} A_{i+1} \rangle & \langle B_{i+r-1} A_{i+3} \rangle & \cdots & \langle B_{i+r-1} A_{i+r} \rangle \end{vmatrix}. \quad (25)$$

Next we turn to the longitudinal component of the spin correlations function, which can be expressed as

$$\langle S_i^z S_{i+r}^z \rangle = \left(\frac{1}{4}\right) \begin{vmatrix} \langle A_i B_i \rangle & \langle A_i B_{i+r} \rangle \\ \langle A_{i+r} B_i \rangle & \langle A_{i+r} B_{i+r} \rangle \end{vmatrix}, \quad (26)$$

the transverse component is given by

$$\langle S_i^x S_{i+r}^x \rangle = \left(\frac{1}{4}\right) \times \begin{vmatrix} \langle B_i A_{i+1} \rangle & \langle B_i A_{i+2} \rangle & \cdots & \langle B_i A_{i+r} \rangle \\ \langle B_{i+1} A_{i+1} \rangle & \langle B_{i+1} A_{i+2} \rangle & \cdots & \langle B_{i+1} A_{i+r} \rangle \\ \vdots & \vdots & \ddots & \vdots \\ \langle B_{i+r-1} A_{i+1} \rangle & \langle B_{i+r-1} A_{i+2} \rangle & \cdots & \langle B_{i+r-1} A_{i+r} \rangle \end{vmatrix}. \quad (27)$$

## IV. RESULTS

In order to check the accuracy to which we can recover the exponents of the clean system we first display all correlations functions for the pure model in a log-log plot in Fig. 1. In the pure model, at zero temperature, Lieb, Schultz and Mattis<sup>25</sup> showed that  $C^z(r)$  is identically zero for  $r$  even, but decays with an exponent of 2 at large  $r$  (odd). Later McCoy<sup>26</sup> showed that  $C^x(r)$  decays with an exponent equal to  $1/2$ . For the pure model  $O^z$  will equal  $C^x$  and  $O^x$  is the square root of  $O^z$  (see Eq. (A12)). Hence  $O^z$  and  $O^x$  will decay with exponents  $1/2$  and  $1/4$  respectively. By using a linear fit to the data points for the three largest system sizes the expected decay exponents are recovered to five significant digits (see Table I).

We next add flat disorder, described by Eq. (2), and expect to see the RS exponent<sup>2</sup> for the spin correlations  $C^x$  and  $C^z$ .  $O^x$  maps on to the transverse field Ising model correlator, which falls off with an exponent of 0.382 in the RS phase<sup>1</sup>. We therefore expect both  $O^x$  and  $O^z$  to fall off with exponent 0.382. We plot the results in Fig. 2.

$C^z$  has previously been reported<sup>11,14</sup> to show algebraic decay with an exponent of 2, as predicted by the RS calculation, and we confirm this result. While  $C^z$  remains the same in the clean and RS case, the exponent of the transverse correlation function  $C^x$  is predicted to change from  $1/2$  in the clean case to 2 in the RS phase. Previous numerical results<sup>11</sup> for  $C^x$  indicated a transition to exponential decay. Contrary to this, our results in Fig. 2 do support an exponent of 2 in the RS case. The exponent appears to be slightly smaller than 2 for the smaller system sizes, but the slope gets very close to 2 for the larger system sizes. We believe that we do not see the correct exponent for smaller system sizes because  $C^x$  has not yet converged to its thermodynamic limit. The last data point ( $N = 1024$ ) is not reliable, since for this large system size and strong disorder the numerical routines have begun to become unstable, and we do not trust the accuracy of this point.

We believe that the exponential decay seen previously was caused by the use of a gaussian distribution of bonds. As the disorder gets strong enough this will introduce ferromagnetic bonds into the system. The ferromagnetic bonds will destroy the antiferromagnetic order leading to the RS phase. Westerberg et al.<sup>6</sup> have shown that the spin 1/2 AF fixed point is unstable towards introduction of FM bonds. Furthermore they showed<sup>7</sup> that the presence of FM bonds leads to exponential decay of the spin correlation function.

We note that although the decay exponent is the same for both components of the correlation functions, the prefactors differ. If the spins were coupled together in pairs as true singlets this would, of course, not be the case. We believe that the different prefactors are caused by residual fluctuations of the valence bonds.

During the course of this work we did fairly extensive studies of various other bond distributions. In particular we worked with a power law distribution

$$P(J) = \alpha J^{-1+\alpha} \theta(J) \theta(1 - J). \quad (28)$$

The motivation for a power law distribution comes from the decimation RG procedure, in which strong bonds in the system form singlets and thereby generate weak induced couplings between their neighbors. This procedure, in effect, eliminates strong bonds and replace them by much weaker bonds. The energy scale is thus lowered and the procedure becomes exact in the low temperature limit<sup>1,4</sup>. After renormalization the bond distribution is given by the above power law distribution. We believed that by starting as close to the fixed point distribution as possible it would be easier to observe the predicted RS behavior of the correlation functions. Another distribution we studied was a flat distribution with mean equal to one, but width less than two. With neither of these distributions did we observe the RS behavior as clearly as with the distribution presented in this paper. There seems to be two competing factors that influence the results. The power law distribution is very close to the fixed point distribution, but the bonds get distributed over several hundred orders of magnitude and the numerical routines become unstable and give increasingly unreliable results. The flat distribution with width less than two behaves very well numerically, but it is far from the fixed point, and we did not manage to reach system sizes large enough to observe the expected behavior. It appears that a flat distribution with mean one and width two is close enough to the fixed point for us to see the RS exponents, but it is not so broad that it causes problems for the numerical routines, except at the largest system size (N=1024).

The string correlation functions decay as predicted in the RS phase. The decay exponent of  $O^x$  changes from 0.50 in the pure case to 0.382 in the RS phase, in agreement with earlier observations<sup>10</sup>. Young and Rieger measured the spin correlation function in the transverse-field Ising chain, which maps onto the transverse component

of the string correlation function in the XX model, see Eq. (A9). The decrease in exponent is of interest since the disorder actually causes the correlation function to fall off slower than in the clean case. We do, however, have to keep in mind that we are looking at the average correlation function and not the typical correlation function. The average correlation function is dominated by a few strong couplings between distant spins. Such strong couplings are a characteristic of the RS phase. The typical correlation function, on the other hand, shows a very different behavior<sup>1-3</sup> and will be studied below. We do also see the predicted change in  $O^z$ , which changes from exponent 0.25 in the pure case to 0.382 in the RS phase.  $O^z$  is the square of  $O^x$  and it is interesting that the disorder average of both quantities decay with the same exponent. Intuitively this can be understood by considering a correlation function that is dominated by a few strong correlations of order 1, while the rest of the correlations are of order 0. The actual distributions are plotted in Fig. 3.

The typical correlation function, here obtained by exponentiating the disorder average of the logarithm of the correlation function is predicted<sup>1</sup> to decay according to

$$f_{\text{typ}}(r) \propto \exp(-A\sqrt{r}), \quad (29)$$

where A is some nonuniversal constant. By plotting the log of  $C_{\text{typ}}^x$  and  $C_{\text{typ}}^z$  against  $\sqrt{r}$  in Fig. 4 we see that this is indeed the case, and a linear fit to all data points gives the value -1.08 and -3.22 respectively for the nonuniversal constant A above. It is of interest to note that  $C^x$  and  $O^z$  are identical for the pure model, but in the RS phase  $C^x$  and  $O^z$  decay with different exponents.  $C_{\text{typ}}^x$  and  $O_{\text{typ}}^z$  are, however, again equivalent in the RS phase. This is easily understood by the mapping to the Ising chain. Looking at Eq. (A12) it is clear that  $C^x$  and  $O^z$  differ in the RS phase since  $O_o^x$  and  $O_e^x$  are anti-correlated. This is illustrated in Fig. 5 and provides further evidence for the RS phase since in the RS phase strong bonds can never cross each other, and this means that if  $O_o^x$  is of order unity, then  $O_e^x$  is bound to be small. The typical correlations  $C_{\text{typ}}^x$  and  $O_{\text{typ}}^z$  are equivalent since

$$\ln(C^x(N/2)) = \ln(O_o^x(N/2 - 1)) + \ln(O_e^x(N/2 - 1)), \quad (30)$$

and because if there is no dimerization in the system the average of  $\ln O_o^x(i - j)$  will equal the average of  $\ln O_e^x(i - j)$ . We note that since  $O^z = (O^x)^2$  the logarithms of the typical correlations  $O_{\text{typ}}^z$  and  $O_{\text{typ}}^x$  will differ by a factor 2.

The distributions of the logarithm of the correlation functions

$$\ln(f(r))/\sqrt{r} \quad (31)$$

is supposed to scale to a fixed distribution for large  $r$ . Young and Rieger<sup>10</sup> studied this distribution for  $O^x$ , and

we present results for  $O^z$  and  $C^x$  in Fig. 6 and Fig. 7. As we see the distributions scale well. The distributions of  $O^z$  and  $C^x$  are very different, and it not obvious from looking at the plots that the typical correlations  $O_{\text{typ}}^z$  and  $C_{\text{typ}}^x$  turn out to be the same (though they do).

Next we focus on a dimerized system with no disorder. Any observable is a function of the three length scales in the system: the system size  $N$ , the distance around the ring  $r$ , and the correlation length  $\xi$ . We make the standard finite size scaling hypothesis and assume that near the critical point ( $\xi = \infty, N = \infty$ ) we can express our observable in terms of a scaling function with dimensionless arguments formed by ratios of our length scales. Hence a correlation function  $C$  can be expressed as

$$C(N, r, \xi) \propto N^\omega f(N/r, N/\xi), \quad (32)$$

where  $\omega$  is a scaling exponent and  $f(N/r, N/\xi)$  is the scaling function. If we measure  $C$  for different system sizes, but at a fixed ratio  $N/r$  and plot  $CN^{-\omega}$  vs.  $N/\xi$  the curves should collapse onto a single scaling function  $f(N/\xi)$ , independently of the values of  $N$  and  $\xi$ . If one assumes that  $N$  is large enough so that  $C$  is not a function of  $N$ , then one can alternatively use data for one system size  $N$ , and different  $r$  and plot  $Cr^{-\omega}$  versus  $r/\xi$ . Again the curves should collapse onto a single scaling function  $f(r/\xi)$ , independently of the values of  $r$  and  $\xi$ , but only as long as the value of  $C$  has reached its thermodynamic limit. This was done by Young and Rieger<sup>10</sup>, but in this paper we present data for different system sizes at a fixed distance half way around the ring,  $r = N/2$ , so that the first argument of the scaling function  $f$  is fixed at  $N/r = 2$ .

Consider the string correlation function  $O_d^x(n, \delta)$  to be a function of the dimerization  $\delta$  and  $n = N/2$ . From above we know that

$$O_d^x(n, \delta = 0) \propto n^{-\frac{1}{4}} \quad (33)$$

and Pfeuty<sup>27</sup> showed that (using the mapping from the XY model to the Ising chain studied by Pfeuty)

$$O_d^x(n = \infty, \delta) \propto \delta^{\frac{1}{4}}. \quad (34)$$

The correlation length for free fermions is of the form  $\xi \propto \delta^{-1}$ . Consider a string correlation function of the form

$$O_d^x(n, \delta) \propto n^\omega f(n\delta). \quad (35)$$

Eq. (34) requires that for asymptotically large values of  $x$ ,  $f(x)$  behaves as  $x^{\frac{1}{4}}$ , which fixes  $\omega$  to  $-\frac{1}{4}$ . We thus expect a single curve when  $O_d^x n^{\frac{1}{4}}$  is plotted versus  $n\delta$ . In Fig. 8 a log-log plot of the scaling function shows that this is indeed the case. For small values of the argument the function is linear,  $f(x) \propto x$ , but for larger values of the argument there is a sharp transition to the asymptotic behavior,  $f(x) \propto x^{\frac{1}{4}}$ . As the dimerization gets too big we notice that there are corrections to scaling.

Since the longitudinal component of the string correlation is the square of the transverse component, the above arguments are identical for  $O_d^z(N, \delta)$ , except that all exponents equal to  $1/4$  are changed to  $1/2$ . The spin correlation function  $C^x$  also scales very well with exponent  $1/2$ , as shown in Fig. 9. The longitudinal spin correlation  $C^z$  shows fairly large corrections to the scaling (see Fig. 10), but the corrections are due to the fact that the correlation is measured at  $r = N/2 - 1$  instead of at  $r = N/2$ . This was checked by plotting the same results for system sizes with  $N/2$  odd, in which case  $C^z$  can be measured at  $r = N/2$ , and there are no visible correction to scaling. But in order to be consistent throughout this paper we have only shown data for system sizes with  $N/2$  even.

If we now add disorder to the dimerized system we expect the correlation length to be of the form<sup>2</sup>  $\xi \propto \delta^{-2}$ . Furthermore we expect that

$$O_d^z(n, \delta = 0) \propto n^{-0.382} \quad (36)$$

Therefore the scaling function for both components of the string correlation function should read

$$O_d^{x,z}(n, \delta) \propto n^{-0.382} f(N\delta^2) \quad (37)$$

In Fig. 11 and Fig. 12 we plot the scaling functions for  $O_d^z$  and  $O_d^x$ . In both cases we see a transitions from  $f(x) \propto x^{\frac{1}{2}}$  to  $f(x) \propto x^{0.382}$ . The transition is not as sharp as in the clean case, and it would be of interest to have reliable data for even larger system sizes.

The average spin correlation functions should scale according to

$$C^{x,z}(n, \delta) \propto n^{-2} f(n\delta^2), \quad (38)$$

but since the critical correlations functions have not reached their asymptotic behavior at the system sizes considered we compensate by plotting  $C^{x,z}(n, \delta)/C^{x,z}(n, \delta = 0)$  vs.  $f(n\delta^2)$ , which works well, as can be seen in Fig. 13 and Fig. 14.

The typical correlation functions are expected to scale as

$$f_{\text{typ}}(n, \delta)/f_{\text{typ}}(n, \delta = 0) \propto f(n/\xi_{\text{typ}}), \quad (39)$$

where  $\xi_{\text{typ}} \propto \delta^{-1}$  in the RD phase. The string correlation functions  $O_{o,\text{typ}}^z$  and  $O_{e,\text{typ}}^x$  appear to follow this scaling behavior fairly well, see Fig. 15 and Fig. 16, but the typical spin correlation functions in Fig. 17 and Fig. 18 show quite dramatic corrections. If we assume that  $\xi_{\text{typ}} \propto \delta^{-1.3}$  the scaling works well, as shown in Fig. 19. We are not sure if this discrepancy with theory is only an effect of large corrections to scaling, or if there is some other reason.

## V. CONCLUSION

We have done extensive numerical simulations of the disordered XX model, using a mapping to free fermions. The decay exponents of the string and spin correlation functions in the RS and RD phases, predicted by RG calculation, have been found in very good agreement with numerical data. In particular the transverse component of the spin correlation function is observed to decay algebraically with the correct decay exponent, as opposed to exponentially as previously observed<sup>11</sup>. We explain this difference in terms of the bond distribution and the introduction of ferromagnetic bonds in the previous study. We also discuss the results of various other bond distributions, emphasizing the importance of being close to the fixed point distribution, but making sure that the numerical routines still give reliable results. Full finite size scaling cross over functions were presented for the longitudinal and transverse components of the average and typical spin and string correlation function in the RD phase, as well as for the pure dimerized model. Only the transverse component of the string correlation function has previously been studied in this manner<sup>10</sup>. In appendix A various relations between the different correlation functions are derived using a mapping to the Ising model in a transverse field. Due to the well-known mapping to free fermions, and the use of parallel computers, disorder averages could be taken over system sizes up to 1024 sites, about ten times larger than in previous studies we are aware of.

We are extremely grateful to Ross Hyman, Senthil Todadri and Kun Yang for their many comments and generous help. We acknowledge support from the NSF grant DMR 97-14055, NSF CDA-9601632 and Ella och Georg Ehrnrooths stiftelse.

### APPENDIX A: TRANSFORMATION TO DECOUPLED ISING CHAINS

We can gain considerable insight into the behavior of, and relationship between various correlation functions by transforming the XY chain into two decoupled Ising chains. Following Fisher we use the following transformation:

$$\begin{aligned}\sigma_n^x &= \prod_{j \leq n} S_j^x \\ \sigma_n^y &= S_n^y S_{n+1}^y \\ \sigma_n^z &= \frac{2}{i} \sigma_n^x \sigma_n^y = \frac{2}{i} \prod_{j \leq n} S_j^x S_n^y S_{n+1}^y.\end{aligned}\tag{A1}$$

The inverse transformation is given by

$$\begin{aligned}S_n^x &= \sigma_{n-1}^x \sigma_n^x \\ S_n^y &= \prod_{j \leq n-1} \sigma_j^y\end{aligned}\tag{A2}$$

$$S_n^z = \frac{2}{i} S_n^x S_n^y = \frac{2}{i} \prod_{j \leq n-1} \sigma_j^y \sigma_{n-1}^x \sigma_n^x.$$

The Hamiltonian is transformed into two decoupled Ising chains:

$$H = \sum_{i=1}^N J_i (S_i^x S_{i+1}^x + S_i^y S_{i+1}^y) = \sum_{i=1}^N J_i (\sigma_{i-1}^x \sigma_{i+1}^x + \sigma_i^y).\tag{A3}$$

The two chains are dual to each other and in the pure dimerized case one chain has coupling constant  $J_o$  and transverse field  $J_e$ , while the other chain has coupling constant  $J_e$  and transverse field  $J_o$ .

Next we look at how the string correlation functions transforms:

$$O^x(r) = \langle S_i^x S_{i+1}^x \cdots S_{i+r}^x \rangle = \langle \sigma_{i-1}^x \sigma_{i+r}^x \rangle.\tag{A4}$$

If  $r$  is even then  $\sigma_{i-1}^x$  and  $\sigma_{i+r}^x$  will belong to different chains and the expectation value  $\langle \sigma_{i-1}^x \sigma_{i+r}^x \rangle = \langle \sigma_{i-1}^x \rangle \langle \sigma_{i+r}^x \rangle$  will vanish. If  $r$  is odd  $O^x(r)$  transforms to the Ising correlator:  $O^x(r) = \langle \sigma_{i-1}^x \sigma_{i+r}^x \rangle$ . The  $y$  component becomes (for  $r$  odd):

$$O^y(r) = \langle S_i^y S_{i+1}^y \cdots S_{i+r}^y \rangle = \langle \sigma_i^y \sigma_{i+2}^y \cdots \sigma_{i+r-1}^y \rangle.\tag{A5}$$

The expectation values of  $O^x$  and  $O^y$  have to be identical and hence

$$\langle \sigma_{i-1}^x \sigma_{i+r}^x \rangle = \langle \sigma_i^x \sigma_{i+2}^x \cdots \sigma_{i+r-1}^x \rangle.\tag{A6}$$

This relates the expectation value of a correlation function on one chain to the expectation value of another correlation function on the other chain.

The  $z$  component of the string correlation function transforms ( $r$  odd) as

$$O^z(r) = \langle S_i^z S_{i+1}^z \cdots S_{i+r}^z \rangle = \langle \sigma_{i-1}^x \sigma_i^y \sigma_{i+2}^y \cdots \sigma_{i+r-1}^y \sigma_{i+r}^x \rangle.\tag{A7}$$

Using the above equality we find that

$$\begin{aligned}O^z(r) &= \langle \sigma_{i-1}^x \sigma_{i+r}^x \rangle \langle \sigma_i^y \sigma_{i+2}^y \cdots \sigma_{i+r-1}^y \rangle \\ &= \langle \sigma_{i-1}^x \sigma_{i+r}^x \rangle^2 = O^x(r)^2,\end{aligned}\tag{A8}$$

and interestingly enough the transverse component of the string order is simply the square of the longitudinal component.

Turning to the spin correlation function we find that

$$C^x(r) = \langle S_i^x S_{i+r}^x \rangle = \langle \sigma_{i-1} \sigma_i \sigma_{i+r-1} \sigma_{i+r} \rangle.\tag{A9}$$

Hence

$$C^x(r) = \begin{cases} \langle \sigma_{i-1} \sigma_{i+r} \rangle \langle \sigma_i \sigma_{i+r-1} \rangle, & \text{if } r \text{ odd} \\ \langle \sigma_{i-1} \sigma_{i+r-1} \rangle \langle \sigma_i \sigma_{i+r} \rangle, & \text{if } r \text{ even.} \end{cases}\tag{A10}$$

The criterion that  $C^x = C^y$  gives us back Eq. (A6). The z component of the spin correlation transforms to

$$C^z(r) = \begin{cases} \langle \sigma_{i-1}^x \sigma_{i+2}^y \sigma_{i+4}^y \cdots \sigma_{i+r-2}^y \sigma_{i+r}^x \rangle \times \\ \langle \sigma_i^x \sigma_{i+2}^y \sigma_{i+4}^y \cdots \sigma_{i+r-2}^y \sigma_{i+r}^x \rangle, & \text{if } r \text{ odd} \\ \langle \sigma_{i-1}^x \sigma_{i+2}^y \sigma_{i+4}^y \cdots \sigma_{i+r-2}^y \sigma_{i+r}^x \rangle \times \\ \langle \sigma_i^x \sigma_{i+2}^y \sigma_{i+4}^y \cdots \sigma_{i+r-2}^y \sigma_{i+r}^x \rangle, & \text{if } r \text{ even} \end{cases} \quad (\text{A11})$$

To summarize we want to emphasize a few important relations between various correlation functions. These equalities follow directly from the fact that the XY chain separates into two decoupled Ising chains. The expressions are obtained by using the above transformations and assuming that  $N/2$  is even, which is the case in our simulations. The relations are:

$$\begin{aligned} C^x(N/2) &= O_o^x(N/2 - 1)O_e^x(N/2 - 1) \\ O_o^z(N/2 - 1) &= (O_o^x(N/2 - 1))^2 \\ O_e^z(N/2 - 1) &= (O_e^x(N/2 - 1))^2. \end{aligned} \quad (\text{A12})$$

- <sup>22</sup> S. M. Girvin and D. P. Arovas, *Physica Scripta* **T27**, 156 (1989); D. P. Arovas and S. M. Girvin, "Exact Questions to Some Interesting Answers in Many Body Physics", *Proc. VIIth Int. Conf. on Recent Progress in Many-Body Theories*, (Plenum Press, New York, 1992), pp. 315-344, editors T.L. Ainsworth, C.E. Campbell, B.E. Clements and E. Kortschek.
- <sup>23</sup> M. Kohmoto and H. Tasaki, *Phys. Rev. B* **46**, 3486 (1992).
- <sup>24</sup> E. Fradkin, *Field Theories of Condensed Matter Systems*, (Addison-Wesley Pub. Co., Redwood City, CA., 1991).
- <sup>25</sup> Elliot Lieb, Theodore Schultz and Daniel Mattis, *Ann. of Phys.* **16**, 407, 1961.
- <sup>26</sup> Barry M. McCoy, *Phys. Rev.* **173**, 531 (1968).
- <sup>27</sup> Pierre Pfeuty, *Ann. of Phys.* **57**, 79 (1969).

	no disorder	RS phase
$C^z$	2 [2.00003(1)]	2
$C^x$	1/2 [0.499998(1)]	2
$O^z$	1/2 [0.499998(1)]	0.382
$O^x$	1/4 [0.249999(2)]	0.382

TABLE I. Decay exponents for the XX spin-1/2 chain, values obtained by linear fit to data in Fig. 1 in brackets.

- <sup>1</sup> Daniel S. Fisher, *Phys. Rev. Lett.* **69**, 534 (1992).
- <sup>2</sup> Daniel S. Fisher, *Phys. Rev. B* **50**, 3799 (1994).
- <sup>3</sup> Daniel S. Fisher, *Phys. Rev. B* **51**, 6411 (1995).
- <sup>4</sup> R.A. Hyman, Kun Yang, R.N. Bhatt and S.M. Girvin, *Phys. Rev. Lett.* **76**, 839, (1996).
- <sup>5</sup> R.A. Hyman, Kun Yang, *Phys. Rev. Lett.* **78**, 1783, (1997).
- <sup>6</sup> E. Westerberg, A. Furusaki, M.Sigrist, and P. A. Lee, *Phys. Rev. Lett.* **75**, 4302, (1995).
- <sup>7</sup> E. Westerberg, A. Furusaki, M.Sigrist, and P. A. Lee, *Phys. Rev. B* **55**, 12578 (1997).
- <sup>8</sup> Leon Balents and Matthew P. A. Fisher, *cond-mat/9706069* (1997).
- <sup>9</sup> Ross H. McKenzie, *Phys. Rev. Lett.* **77**, 4804 (1996).
- <sup>10</sup> A.P. Young and H. Rieger, *Phys. Rev. B* **53**, 8486 (1996).
- <sup>11</sup> Heinrich Röder, Joachim Stolze, Richard N. Silver and Gerhard Müller, *J. Appl. Phys.* **79**, 4632 (1996).
- <sup>12</sup> Kazuo Hida, *Phys. Rev. B* **45**, 2207 (1992).
- <sup>13</sup> Kazuo Hida, *cond-mat/9707239* (1997).
- <sup>14</sup> Stephan Haas, Jose Riera and Elbio Dagotto, *Phys. Rev. B* **48**, 13174 (1993).
- <sup>15</sup> M. Guo, R. N. Bhatt and D. A. Huse, *Phys. Rev. Lett.* **72**, 4137 (1994).
- <sup>16</sup> H. Rieger and A. P. Young, *Phys. Rev. B* **54**, 3328 (1996).
- <sup>17</sup> T. Senthil, *cond-mat/9709164* (1997)
- <sup>18</sup> F.D.M. Haldane, *Phys. Lett.* **93A**, 464 (1983).
- <sup>19</sup> R.R.P Singh *et al.*, *Phys. Rev. Lett.* **61**, 2484 (1988).
- <sup>20</sup> S. K. Ma, C. Dasgupta and C-K Hu, *Phys. Rev. Lett.* **43**, 1434 (1979); C. Dasgupta and S. K. Ma, *Phys. Rev. B* **22**, 1305 (1979)
- <sup>21</sup> M. den Nijs and K. Rommelse, *Phys. Rev. B* **40**, 4709 (1989).

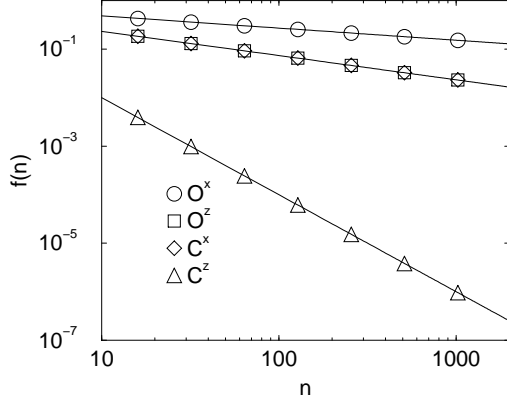


FIG. 1. The spin and string correlations functions in the clean XX model. System sizes go from  $N = 32$  to  $N = 2048$  and  $n = N/2$ . The solid lines are linear fits to the three largest systems. Slopes are given in Table I.

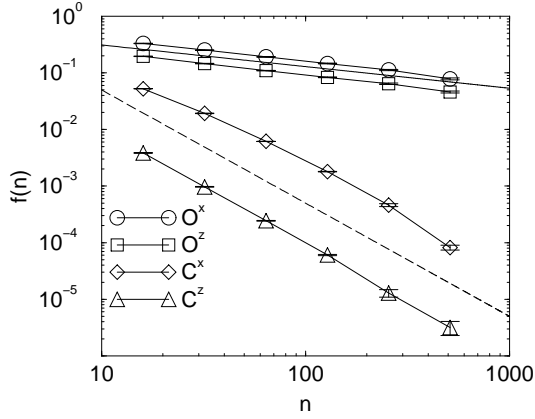


FIG. 2. The spin and string correlation functions in the disordered XX model. Disorder averages are taken over  $5 \times 10^3 - 10^5$  configurations, and system sizes vary from  $N = 32$  to  $N = 1024$ . The solid and dashed lines have slopes  $-2$  and  $-0.382$  respectively.

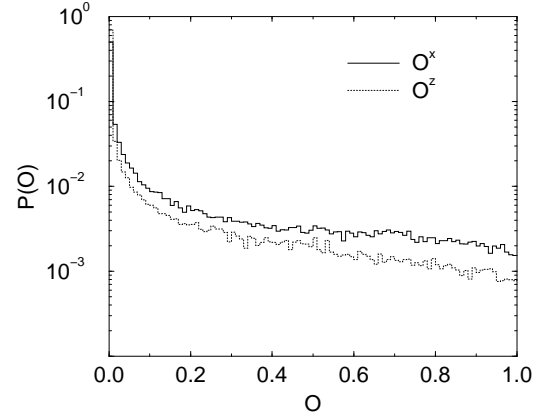


FIG. 3. The distribution of the transverse and longitudinal components of the string correlation function in the RS phase for system size  $N = 256$ .

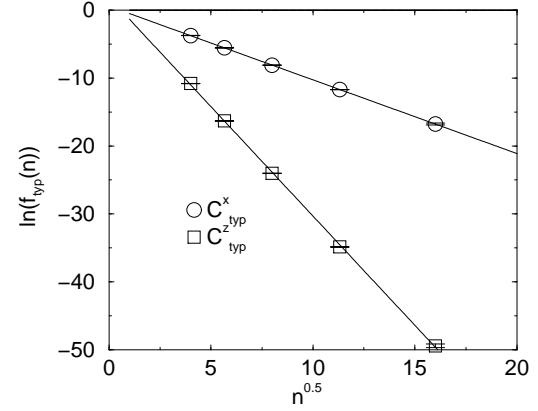


FIG. 4. The typical correlation functions plotted versus the square root of the system size. The solid lines are linear fits to all data points.

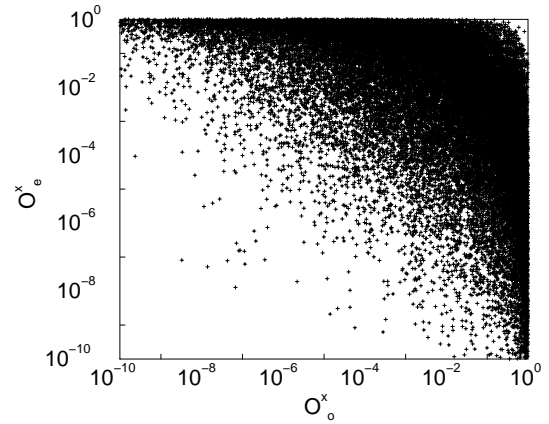


FIG. 5.  $O_e^x$  plotted against  $O_o^x$  in the RS phase for  $N = 256$ .



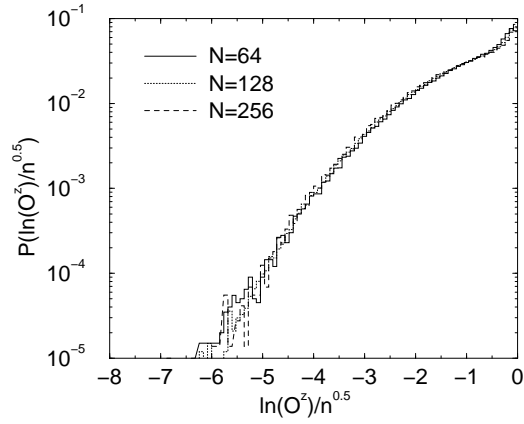


FIG. 6. The distribution of the longitudinal component of the string correlation function in the RS phase.

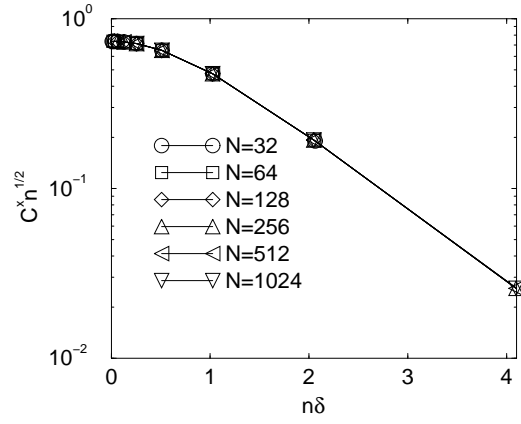


FIG. 9. The transverse component of the spin correlation function in the dimerized XX model.

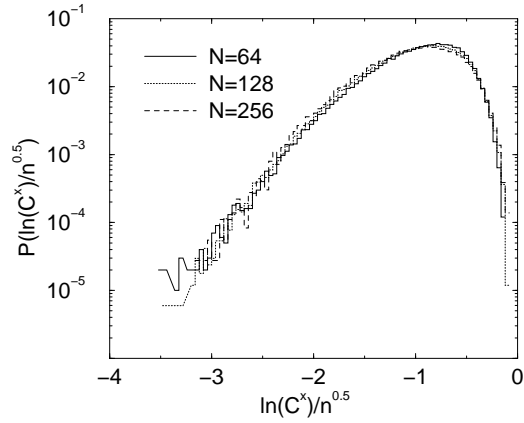


FIG. 7. The distribution of the transverse component of the spin correlation function in the RS phase.

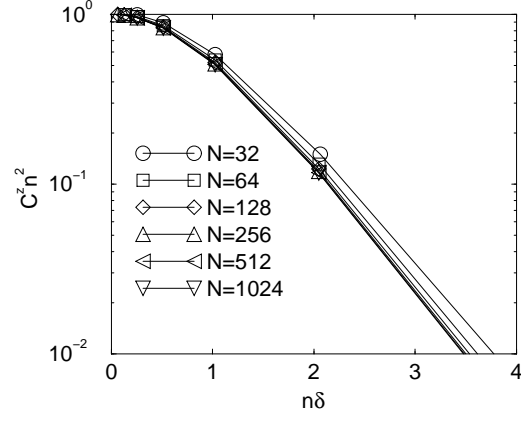


FIG. 10. The longitudinal component of the spin correlation function in the dimerized XX model.

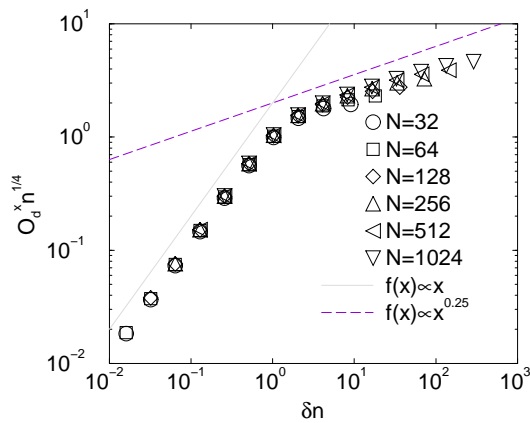


FIG. 8. The transverse component of the string correlation function in the dimerized XX model.

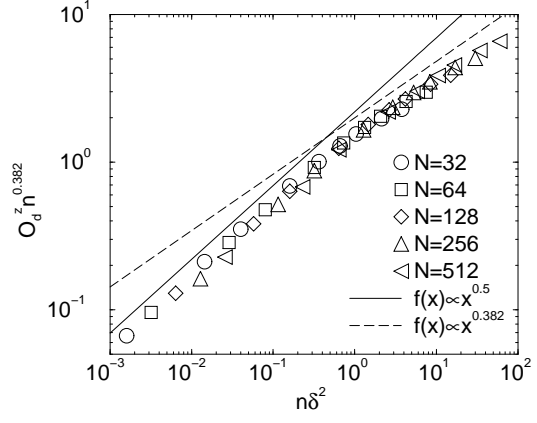


FIG. 11. The longitudinal component of the string correlation function in the dimerized and disordered XX model.

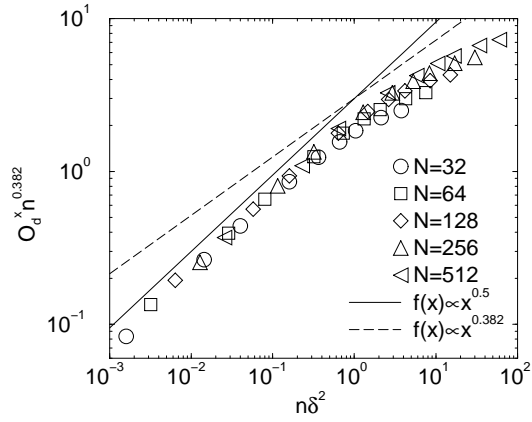


FIG. 12. The transverse component of the string correlation function in the dimerized and disordered XX model.

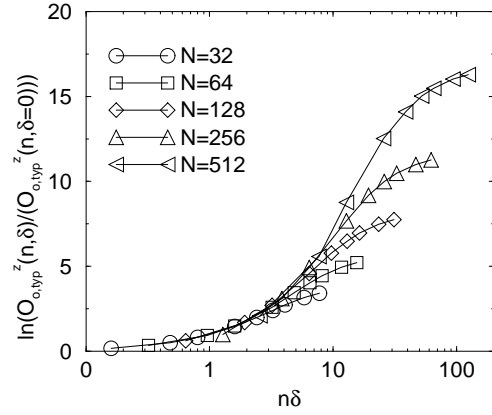


FIG. 15. The longitudinal component of the typical string correlation function in the dimerized and disordered XX model.

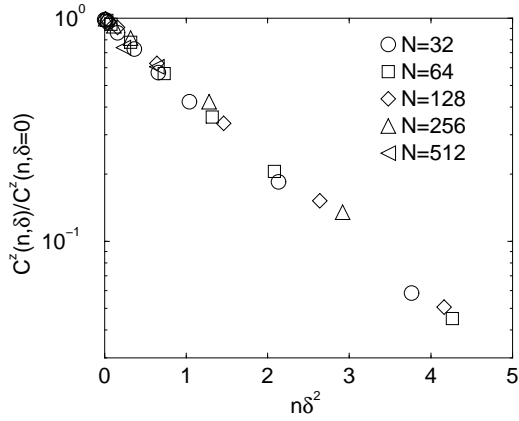


FIG. 13. The longitudinal component of the spin correlation function in the dimerized and disordered XX model.

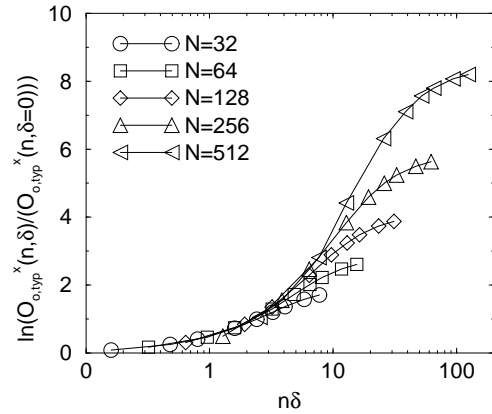


FIG. 16. The transverse component of the typical string correlation function in the dimerized and disordered XX model.

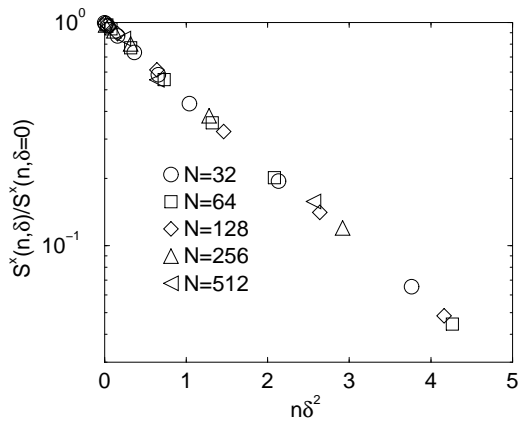


FIG. 14. The transverse component of the spin correlation function in the dimerized and disordered XX model.

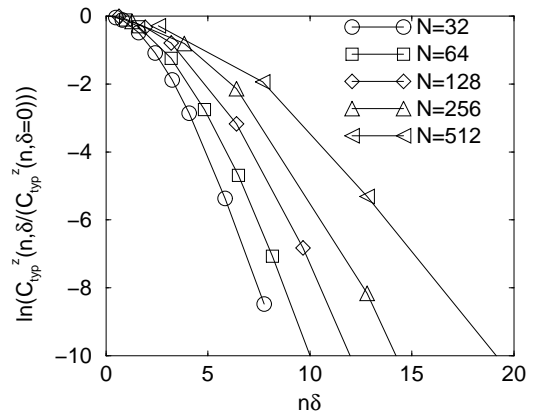


FIG. 17. The longitudinal component of the typical spin correlation function in the dimerized and disordered XX model.

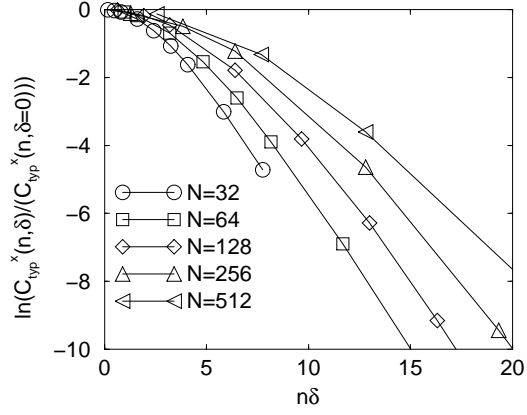


FIG. 18. The transverse component of the typical spin correlation function in the dimerized and disordered XX model.

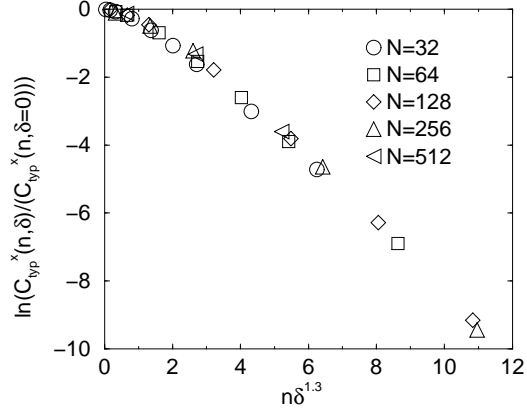


FIG. 19. The transverse component of the typical spin correlation function in the dimerized and disordered XX model, with  $\xi \propto \delta^{1.3}$ .